JACS
JOURNAL OF THE AMERICAN CHEMICAL SOCIETY

ARTICLE

pubs.acs.org/JACS

A Nonemissive Iridium(III) Complex That Specifically Lights-Up the Nuclei of Living Cells

Chunyan Li, Mengxiao Yu, Yun Sun, Yongquan Wu, Chunhui Huang, and Fuyou Li*

Joint Center of Biomedical Imaging (BMI) of Department of Chemistry & Institute of Biomedical Science & Cancer Hospital, Laboratory of Advanced Materials, Fudan University, Shanghai 200433, P. R. China

Supporting Information

ABSTRACT: A nonemissive cyclometalated iridium(III) solvent complex, without conjugation with a cell-penetrating molecular transporter, $[Ir(ppy)_2(DMSO)_2]^+PF_6^-$ (**LIr1**), has been developed as a first reaction-based fluorescence-turn-on agent for the nuclei of living cells. **LIr1** can rapidly and selectively light-up the nuclei of living cells over fixed cells, giving rise to a significant luminescence enhancement (200-fold), and shows very low cytotoxicity at the imaging concentration (incubation time <10 min, LIr1 concentration 10 μM). More importantly, in contrast to the reported nuclear stains that are based on luminescence enhancement through interaction with nucleic acids, complex **LIr1** as a nuclear stain has a reaction-based mode of action, which relies on its rapid reaction with histidine/histidine-containing proteins. Cellular uptake of **LIr1** has been investigated in detail under different conditions, such as at various temperatures, with hypertonic treatment, and in the presence of metabolic and endocytic inhibitors. The results have indicated that **LIr1** permeates the outer and nuclear membranes of living cells through an energy-dependent entry pathway within a few minutes. As determined by an inductively coupled plasma atomic emission spectroscopy (ICP-AEC), **LIr1** is accumulated in the nuclei of living cells and converted into an intensely emissive adduct. Such novel reaction-based nuclear staining for visualizing exclusively the nuclei of living cells with a significant luminescence enhancement may extend the arsenal of currently available fluorescent stains for specific staining of cellular compartments.

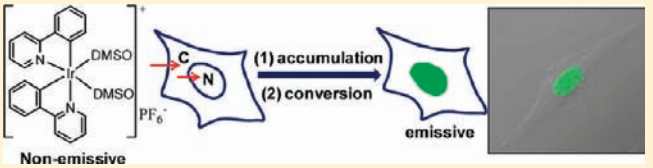

INTRODUCTION

The cell nucleus, the most conspicuous organelle in the eukaryotic cell, houses the chromosomes and controls metabolism, heredity, and reproduction.[1] Since visualization of these nucleus-related events by fluorescence microscopy is very important for biomedical studies, a great deal of attention has been paid to developing fluorescent nuclear stains. Currently, some small-molecular dyes are being used as commercial nuclear imaging agents.[2] Two representative examples are the fluorescent cationic dyes 4′,6-diamidino-2-phenylindole (DAPI, λ_{exc} = 364 nm, λ_{em} = 454 nm) and Hoechst 33342 (λ_{exc} = 352 nm, λ_{em} = 461 nm). These organic dyes, the fluorescence of which is quenched by hydrogen bonding with water, bind to nucleic acids and intercalate among their stacked base pairs, leading to a fluorescence enhancement in the nuclear region. These commercial organic dyes usually require ultraviolet (UV) light as excitation light source, which can lead to extensive cellular damage and significant autofluorescence from biological samples.[3]

Metal-based emissive probes (including lanthanide complexes[4,5] and heavy-metal complexes[6,7]) are interesting alternatives, because they exhibit advantageous photophysical properties for bioimaging, such as enhanced photostability,[8] and large Stokes shifts for easy distinction between emission and excitation.[9] More importantly, these materials possess relatively long lifetimes (~μs and ms), and hence become appealing as probes that could completely eliminate short-lived autofluorescence (~ns) through a time-resolved technique.[10] Recently, Parker et al. reported an interesting Tb complex bearing two trans-related azaxanthone chromophores, which selectively stained the nuclei of cells, allowing the monitoring of nuclear DNA changes in dividing cells in the course of mitosis.[11] Barton et al. developed a phosphorescent ruthenium complex conjugated with a cell-penetrating peptide to facilitate entry to the nucleus,[12] and Thomas et al. reported a dinuclear ruthenium(II) polypyridyl complex as a luminescent agent that stained the nuclear DNA of living cells.[13]

It should be noted that the above-mentioned luminescent dyes permeate the outer and nuclear membranes of cells nonselectively and exhibit a fluorescence enhancement when they are intercalated between the stacked base pairs of nucleic acids in the nuclear region. That is to say, the design of nuclear imaging agents is still focused on dyes that bond to nucleic acids and serve as a "light-switch" for DNA. In contrast to this nucleic acid-bonding strategy, we demonstrate herein a new design strategy that does not involve bonding to nucleic acids to fabricate a nonemissive reaction-based dye for visualizing exclusively the nuclei of living cells with a significant luminescence enhancement. The nonemissive cyclometalated iridium(III) solvent complex $[Ir(ppy)_2(DMSO)_2]^+PF_6^-$ (**LIr1**), without conjugation of a molecular transporter, can react with histidine and histidine-rich proteins to exhibit intense emission, thereby selectively lighting-up the nuclei of living cells very quickly. Furthermore, the

Received: March 15, 2011
Published: June 17, 2011

interactions of **LIr1** with a series of biomolecules, and the dependence of its cellular uptake on different conditions, such as low temperature, hypertonic treatment, and the presence of metabolic and endocytic inhibitors, have been investigated in detail. We present evidence for an energy-dependent entry pathway for the cellular uptake of **LIr1** and a non-nucleic acid-bonding mechanism for nucleus staining.

EXPERIMENTAL SECTION

Materials and General Instruments. 2-Phenylpyridine (ppy), 2-ethoxyethanol, phosphate buffered saline (PBS), DMSO, L-alanine (Ala), L-arginine (Arg), L-asparagine (Asp), L-glutamine (Gln), L-glycine (Gly), L-isoleucine (Ile), L-leucine (Leu), L-lysine (Lys), L-phenylalanine (Phe), L-proline (Pro), L-serine (Ser), L-threonine (Thr), L-tryptophan (Try), L-tyrosine (Tyr), L-valine (Val), L-glutamic acid (Glu), L-cysteine (Cys), L-methionine (Met), L-histidine (His), lysozyme, bovine serum albumin (BSA), deoxyribonucleotide triphosphate (dNTP), and CT DNA were obtained from Acros. $IrCl_3 \cdot 3H_2O$ was an industrial product and used without further purification. Polypeptides including 6×His, Pro-Cys-Asn-Glu-Met-Leu, Arg-Trp-Ser-Asp-Thr-Tyr, and Val-Gly-Ala-Lys-Gln-Phe were purchased from Shanghai Bootech Bioscience and Technology Co., Ltd. Hoechst 33258, propidium iodide (PI), and cell culture reagents were purchased from Invitrogen. Metabolic inhibitors (oligomycin, deoxyglucose) and endocytosis inhibitor (chloroquine) were obtained from Sigma-Aldrich.

^{1}H NMR spectra were recorded with a Varian spectrometer at 400 MHz. Electrospray ionization mass spectra (ESI-MS) were measured on a Micromass LCTTM system. UV−visible spectra were recorded on a Shimadzu UV-2550 spectrometer. Steady-state emission experiments at room temperature were measured on an Edinburgh instrument FL-900 spectrometer with Xe lamp as excitation source. Luminescence lifetime studies were performed with an Edinburgh FL-900 photocounting system with a hydrogen-filled lamp as the excitation source. Luminescence quantum yields of **1**-histidine in aerated solution were measured with reference to quinine sulfate (0.55 in 0.05 M H_2SO_4).

Synthesis of Iridium(III) Complex LIr1. The complex **LIr1** was synthesized according to previously reported methods.[14−16] Briefly, a mixture of 2-ethoxyethanol and water (3:1, v/v) was added to a flask containing $IrCl_3 \cdot 3H_2O$ (1 mmol) and ppy (2.5 mmol). The mixture was refluxed for 24 h. On cooling, a yellow precipitate was deposited, which was collected by filtration and identified as $[(ppy)_2Ir(\mu\text{-}Cl)_2Ir(ppy)_2]$. This dimer was used for the next reaction without further purification. Thus, a mixture of $[(ppy)_2Ir(\mu\text{-}Cl)_2Ir(ppy)_2]$ (0.085 g, 0.079 mmol) and DMSO (30 mL) was heated to reflux. After 2 h, the yellow solution was cooled to room temperature, whereupon a 4-fold excess of potassium hexafluorophosphate was added. The suspension was stirred for 1 h and then filtered to remove insoluble inorganic salts. The filtrate was concentrated to dryness under reduced pressure. The crude product obtained was chromatographed on silica eluting with CH_2Cl_2/acetone (15:1) to afford $[Ir(ppy)_2(DMSO)_2]^+PF_6^-$ in 47% yield as a yellow solid, which was characterized by ^{1}H NMR and ESI-MS measurement. ^{1}H NMR (400 MHz, DMSO-d_6, TMS): δ = 9.78 (d, J = 6.0 Hz, 2), 9.51 (d, J = 5.2 Hz, 2′), 8.24 (d, J = 7.6 Hz, 5), 8.16 (d, J = 8.4 Hz, 5′), 8.07 (t, J = 7.2 Hz, J = 7.6 Hz, 4), 7.99 (t, J = 7.6 Hz, J = 8.0 Hz, 4′), 7.76 (d, J = 7.2 Hz, 6), 7.71(d, J = 7.6 Hz, 6′), 7.55 (t, J = 6.0 Hz, J = 6.8 Hz, 3), 7.43 (t, J = 6.0 Hz, J = 6.8 Hz, 3′), 6.87 (t, J = 7.2 Hz, J = 8.0 Hz, 7), 6.82 (t, J = 7.6 Hz, 8), 6.74 (t, J = 7.6 Hz, 8′), 6.67(t, J = 8.0 Hz, J = 7.6 Hz, 7′), 6.22 (d, J = 7.2 Hz, 9), 5.64 (d, J = 7.2 Hz, 9′). m/z (ESI-MS, Solvent: DMSO), 657.1, corresponding to $[Ir(ppy)_2(DMSO)_2]^+$.

Interaction of LIr1 with Amino Acids and Biomolecules. The interaction of **LIr1** with amino acids, polypeptides, lysozyme, bovine serum albumin (BSA), deoxyribonucleotide triphosphate (dNTP), and CT DNA has been investigated by luminescent emission titration. Herein, L-alanine (Ala), L-arginine (Arg), L-asparagine (Asp), L-glutamine (Gln), L-glycine (Gly), L-isoleucine (Ile), L-leucine (Leu), L-lysine (Lys), L-phenylalanine (Phe), L-proline (Pro), L-serine (Ser), L-threonine (Thr), L-tryptophan (Try), L-tyrosine (Tyr), L-valine (Val), L-glutamic acid (Glu), L-cysteine (Cys), L-methionine (Met), and L-histidine (His) were used as examples of amino acids. In particular, the absorption and emission responses of **LIr1** to different amount of histidine were studied in detail.

Competitive Binding Assay. The competitive binding of CT DNA and BSA to complex **LIr1** was carried out in a 5 mM Tris-HCl/NaCl buffer (pH 7.4) using luminescence detection. Complex **LIr1** (30 μM) was mixed with CT DNA in a molar ratio of 1:10 and incubated at 25 °C for 1 h in Tris-HCl/NaCl buffer. Then, 10 equiv BSA (300 μM) was added and incubated at 25 °C for another 1 h. The luminescence intensity at 520 nm (λ_{ex} = 365 nm) was measured on an enzyme-linked immunosorbent assay (ELISA) reader (Infinite M200, Tecan, Austria).

Amphiphilicity. The octanol/water partition coefficient, $P_{o/w}$ (or log $P_{o/w}$), is a measure of the amphiphilicity of a material. It represents the relative solubilities of a given material in oil and water. The octanol/water partition coefficient $P_{o/w}$ of **LIr1** was measured on an HY-4 oscillator according to a classical method.[17] Equal amounts of n-octanol and phosphate-buffered saline (PBS) were thoroughly mixed in the oscillator for 24 h. The mixture was then left to separate for a further 24 h so as to yield water and octanol phases, each saturated with the other. Complex **LIr1** was carefully dissolved in PBS (concentration denoted as C_o) and PBS saturated with octanol to form a 20 μM solution. The latter was then mixed with an equal amount of octanol (saturated with water) and shaken again as described above. After separation, the final concentration of **LIr1** in water was denoted as C_w. Both C_o and C_w were measured by spectrophotometry at λ = 310 nm, and the partition coefficient ($P_{o/w}$) for **LIr1** was calculated according to the equation: $P_{o/w} = (C_o - C_w)/C_w$.

Cell Culture. The HeLa and KB lines were provided by the Institute of Biochemistry and Cell Biology, SIBS, CAS (China). Primary mesenchymal stem cells (MSCs) and fibroblast-like synoviocyte (FLS) cell line was presented by the Jiangsu Stem Cell Bank and the State Key Laboratory of Genetic Engineering (SKLGE) in Fudan University, respectively. The HeLa cells were grown in DMEM (Dulbecco's modified Eagle's medium) supplemented with 10% FBS (fetal bovine serum). The KB and FLS cells were grown in RPMI 1640 supplemented with 10% FBS. MSCs were grown in DMEM/F12 supplement with 10% FBS. All cells culture was at 37 °C under 5% CO_2.

Cell Viability/Cell analyzer. HeLa cells (1×10^6 cells) were treated with 10 μM **LIr1** for 10 min. After trypsinization, the cells were washed twice with PBS and cell viability was assessed using a Casy Cell Counter and Analyzer System TT (Schärfe System, Reutlingen, Germany).

Cytotoxicity Assay. The *in vitro* cytotoxicity was measured using a standard methyl thiazolyl tetrazolium (MTT, Sigma-Aldrich) assay in HeLa, KB and FLS cell lines. Briefly, Cells growing in log phase were seeded into 96-well cell-culture plate at 1×10^4/well. The complex **LIr1** (100 μL/well) at concentrations of 20, 40, 60, 80, and 100 μM was added to the wells of the treatment group, and 100 μL/well DMSO diluted in DMEM or RPMI 1640 at final concentration of 0.2% to the negative control group, respectively. The cells were incubated for 24 and 48 h at 37 °C under 5% CO_2. The combined MTT/PBS solution was added to each well of the 96-well assay plate, and incubated for an additional 4 h. An enzyme-linked immunosorbent assay (ELISA) reader (infinite M200, Tecan, Austria) was used to measure the OD570 (Absorbance value) of each well referenced at 690 nm. The following formula was used to calculate the viability of cell growth:

$$\text{Viability}\ (\%) = (\text{mean of Absorbance value of treatment group}/\text{mean Absorbance value of control}) \times 100$$

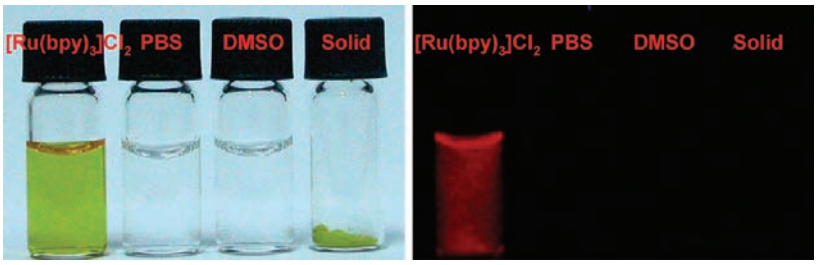

Figure 1. Photographs of the bright-field and room temperature luminescent emissions of **LIr1** (100 μM) in DMSO solution, PBS buffer solution, and as a solid-state powder, with $[Ru(bpy)_3]Cl_2$ as a reference. The excitation wavelength was 365 nm from a portable lamp.

Determination of Iridium(III) Concentration in Cytoplasm and Nucleus. After digestion by trypsin-EDTA solution, HeLa cells were counted and divided into two parts (each part 5×10^6 cells). When the cells adhered to the culture flask, the culture medium was changed to 10 mL of PBS with 10 μM LIr1. The cells were incubated with **LIr1** for 10 min at 37 °C. Thereafter, they were carefully washed with PBS, and then the nuclei and cytoplasm were extracted using a nucleus extraction kit (Nanjing KeyGen Biotech. Co., Ltd.). The iridium concentration in the samples was determined by an inductively coupled plasma atomic emission spectroscopy (ICP-AEC Thermo Elemental Co., Ltd.).

Luminescence Imaging. *For Live Cell Imaging.* Cells (5×10^8/L) were plated on 14 mm glass coverslips and allowed to adhere for 24 h. The cells were washed with PBS and then incubated solely with 10 μM iridium complexes in DMSO/PBS (pH 7.4, 1:99, v/v) for 10 min at 37 or 4 °C. Cell imaging was then carried out after washing the cells with PBS.

For Live Cell Imaging after Treatment with Metabolic and Endocytic Inhibitors. Cells were detached from the culture and were preincubated with 50 mM 2-deoxy-D-glucose and 5 μM oligomycin, with 100 μM chloroquine, or with 50 mM NH_4Cl in PBS, for 1 h at 37 °C. The cells were then washed with PBS and incubated solely with 10 μM **LIr1** in DMSO/PBS (pH 7.4, 1:99, v/v) for 10 min at 37 °C. Before imaging, the cells were washed three times with PBS.

For Colocalization Imaging of Living Cells. The cells were washed with PBS, then incubated with 10 μM LIr1 in DMSO/PBS (pH 7.4, 1:99, v/v) for 10 min at 37 °C, and then further incubated with Hoechst 33258 for another 20 min before imaging.

For Colocalization Imaging of Fixed Cells. The cells were detached from the culture and were fixed with 4% paraformaldehyde at room temperature for 20 min. After washing with PBS, the fixed cells were incubated with 10 μM **LIr1** in DMSO/PBS (pH 7.4, 1:99, v/v) for 10 min at 37 °C, and then further stained with Hoechst 33258 for another 20 min. After washing with PBS, the coverslips were separated from the chamber, and the cells were mounted with 10% glycerol and sealed with nail varnish on a glass substrate.

Luminescence imaging, including *xy*-scan, lambda-scan, T-scan, and time-lapse imaging, was performed with an Olympus FluoView FV1000 confocal fluorescence microscope and a 60× oil-immersion objective lens.[18] Cells incubated with **LIr1** were excited at 488 nm with a semiconductor laser, and the emission was collected at 520 ± 20 nm. Quantization by line plots was accomplished using the software package provided by Olympus instruments. Hoechst 33258 was excited using a laser at 405 nm, and the emission was collected at 460 ± 20 nm. PI was excited using a laser at 488 nm, and the emission was collected at 620 ± 20 nm.

Protein Isolation and Electrophoresis. HeLa cells were maintained in DMEM supplemented with 10% fetal bovine serum (FBS) at 37 °C and 5% CO_2. The cells were harvested and isolation of nuclear and cytoplasmic proteins was performed according to the Nuclear and Cytoplasmic Protein Extraction Kit (Beyotime Biotech, China). The extraction proteins were dissolved in SDS-sample buffer, heated according to the manufacturer's instruction, and then separated using a 5% stacking gel and 12% resolving gel. After electrophoresis, the gels were stained with complex **LIr1** (50 μM) for 20 min. The staining of the gels was measured on the Bio-Rad Gel Doc imaging system.

Cellular Uptake of LIr1 under Hypertonic Conditions. Hypertonic treatment was employed to analyze the effect of **LIr1** diffusion into HeLa cells. Cells were seeded into 96-well cell-culture plates at a density of 2×10^4 cells/well in PBS. A mixture of complex **LIr1** (10 μM) and a combination of sucrose/PBS (w/v) at different concentrations of 1%, 2.5%, 5%, 10%, and 30% was added to each well of the 96-well assay plate. An enzyme-linked immunosorbent assay (ELISA) reader (Infinite M200, Tecan, Austria) was then used to measure the luminescence intensity at 520 nm (λ_{ex} = 365 nm) of each well (n = 3).

Flow Cytometry Analysis. Cellular uptake of **LIr1** (10 μM) under different conditions was assessed by means of flow cytometry (BD FACSCalibur). HeLa cells preincubated with or without 50 mM 2-deoxy-D-glucose and 5 μM oligomycin in PBS for 1 h at 37 °C were incubated with 10 μM **LIr1** in PBS (pH 7.4) for 10 min at 37 or 4 °C. The cells were harvested, rinsed in PBS, resuspended, and determined by flow cytometry.

RESULTS AND DISCUSSION

Synthesis and Photophysical Properties of LIr1. The synthetic procedure for the cationic cyclometalated iridium(III) solvent complex **LIr1** consisted of two steps. First, the chloro-bridged dinuclear iridium(III) precursor $[Ir(dfpy)_2Cl]_2$ was synthesized according to the method reported by Nonoyama.[14] Then, the cationic solvent complex **LIr1** was synthesized by a bridge-splitting reaction of $[Ir(dfpy)_2Cl]_2$ and subsequent complexation with the requisite solvent DMSO. The chemical structure of **LIr1** was further confirmed by ESI-MS (Figure S1 in the Supporting Information). The ESI mass spectrum features a major peak centered at m/z 657.1 corresponding to **LIr1**. The photophysical properties of **LIr1** were also investigated. The UV/vis absorption spectrum of **LIr1** in HEPES buffer solution is shown in Figure S2. **LIr1** displays intense high-energy absorption bands in the region 250−325 nm, and weak bands in the region 330−470 nm that can be assigned to mixed singlet and triplet metal-to-ligand charge-transfer (^{1}MLCT and ^{3}MLCT) and intraligand ($\pi-\pi^*$) transitions (ppy).[19,20] Moreover, like other reported cyclometalated iridium(III) solvent complexes $[Ir(ppy)_2(H_2O)_2]^+$ and $[Ir(ppy)_2(CH_3CN)_2]^+$,[20] **LIr1** exhibits negligible luminescence in both solution and the solid state at room temperature (Figure 1).

Cellular Uptake. Interestingly, after treating living HeLa, KB, FLS, and MSC cells with **LIr1** for 10 min, intense luminescence was detected in the nuclear region under excitation at 488 nm, while the luminescence in the cytoplasm was very weak (Figure 2a). As shown in Figure 2b,c, quantification of the luminescence

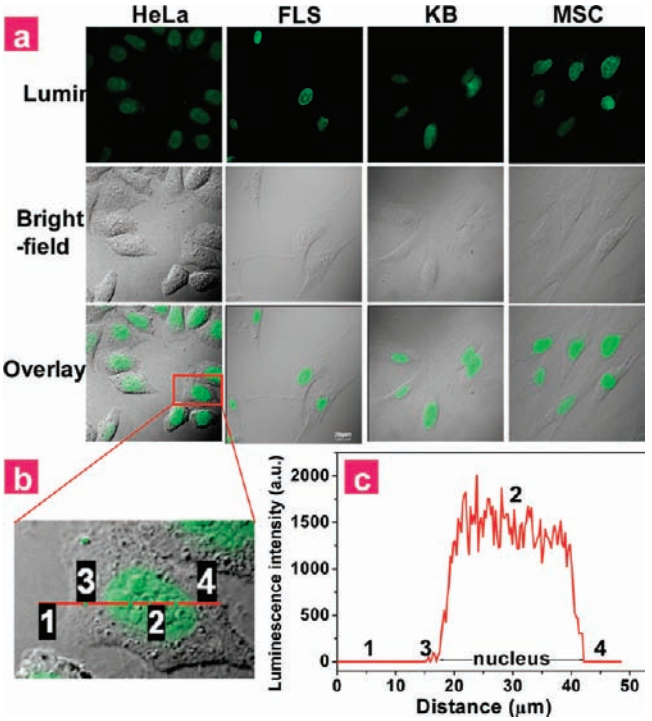

Figure 2. (a) Confocal luminescence images of living HeLa, FLS, KB, and MSC cells incubated with 10 μM **LIr1** in DMSO/PBS (pH 7.4, 1:99, v/v) for 10 min at 37 °C (λ_{ex} = 488 nm, λ_{em} = 520 ± 20 nm). (b) Amplified confocal luminescence imaging (as shown in panel a) of living HeLa cells incubated with 10 μM **LIr1** in DMSO/PBS (pH 7.4, 1:99, v/v) for 10 min at 37 °C. (c) Luminescence intensity profile across the line shown in panel b corresponding to extracellular region (1), nuclear region (2), and cytoplasm (3 and 4).

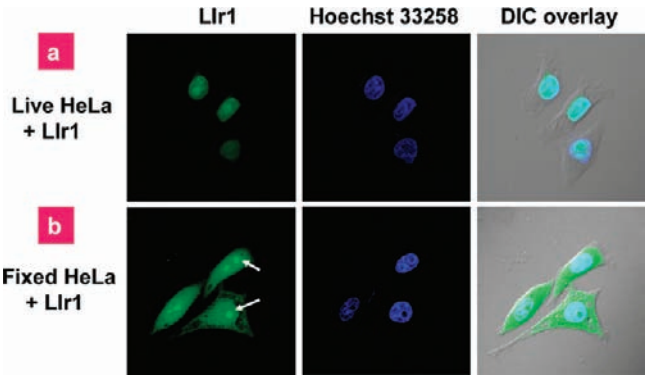

Figure 3. Confocal luminescence images of (a) living HeLa cells incubated with 10 μM **LIr1** in DMSO/PBS (pH 7.4, 1:99, v/v) for 10 min at 37 °C and then further incubated with Hoechst 33258, and (b) fixed HeLa cells stained with **LIr1** and Hoechst 33258 under the same conditions. Arrows point to the nucleolus of HeLa cells.

intensity profile of **LIr1**-treated HeLa cells revealed an extremely high signal ratio between the nucleus (region 2, >1000) and the cytoplasm (regions 3 and 4, ~0), suggesting an exclusive staining of the cell nuclei. This conclusion was further confirmed by complete intracellular colocalization with the nuclear counterstain Hoechst 33258. As shown in Figure 3a, the bright spots (green), that is, the luminescence of **LIr1**, were perfectly colocalized with those (blue) obtained at the setting for Hoechst 33258,

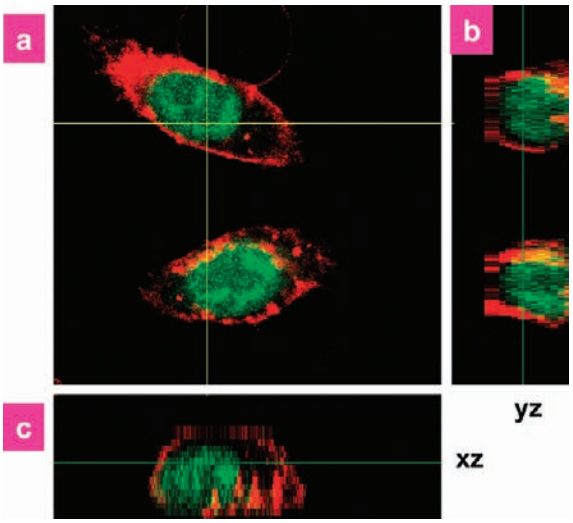

Figure 4. Three-dimensional luminescence images of live KB cells loaded with 10 μM **LIr1** in DMSO/PBS (pH 7.4, 1:99, v/v) for 10 min at 25 °C. The cell membrane was stained red with DiI. Panel a is an *xy* image obtained at z = 7.47 μm, while panels b and c display the *yz* and *xz* cross sections (z = 0.87−16.27 μm) taken at the lines shown in panel a, respectively.

and the colocalization was evident from bright sky-blue spots in the region of the nucleus. Moreover, the nucleolus of the HeLa cells also showed strong luminescence intensity (Figure 3b). These facts indicated that the nonemissive complex **LIr1** acts as a luminescence-enhanced imaging agent for cell nuclei without requiring prior membrane permeabilization.

A further exploration of **LIr1** for nuclear staining was carried out by three-dimensional (3D) visualization of live cells. KB cells were loaded with DiI (for membrane staining) and **LIr1**, and then were imaged by serially scanning at increasing depths along the *z*-axis. As shown in an *xy* image of the cells obtained at a certain depth *z*, the cell membrane is stained red with DiI, while the nuclear regions are also clearly evident owing to staining with **LIr1** (Figure 4a). Interestingly, by virtue of 3D reconstruction of serial *xy* sections, the nuclei of KB cells are perfectly visualized in the *xz* and *yz* cross-sectional images (Figure 4b,c), indicating that the luminescence enhancement occurred in the entire nucleus.

It should be noted that this specific nucleus staining by **LIr1** with a luminescence enhancement effect is not restricted to cancer cell lines, but that cell-specific effects are operative. For example, primary cells lines, FLS and MSC cells, also exhibited intense luminescence in the nuclear region (Figure 2a) when they were incubated with **LIr1**, and high signal ratios (>200, as shown in Figure S5 in the Supporting Information) between the nucleus and the cytoplasm were observed for **LIr1**-treated living FLS and MSC cells. Therefore, we can conclude that **LIr1** can selectively stain the nuclear region in both primary and transformed cell lines. Moreover, the specific nucleus staining by **LIr1** was achieved only for living cells and not for fixed cells. When HeLa cells were fixed and further incubated with **LIr1**, a generalized diffuse whole-cell staining pattern was observed by confocal luminescence bioimaging (Figure 3b), which is significantly different from the specific nucleus staining seen in living cells (Figure 3a).

Cytotoxicity of Complex LIr1. The long-term cellular toxicity of **LIr1** toward the HeLa, KB, and FLS cell lines was determined by means of an MTT assay. In the presence of an LIr1 concentration

Table 1. ***In Vitro*** **Cytotoxicity of LIr1 by MTT Assay**[a]

concentration	24 h			48 h		
(μM)	HeLa	KB	FLS	HeLa	KB	FLS
0	100	100	100	100	100	100
20	98.8 ± 3.9	98.7 ± 4.1	98.4 ± 2.3	98.3 ± 2.3	98.3 ± 2.1	98.2 ± 3.3
40	98.4 ± 3.1	98.4 ± 1.0	97.6 ± 2.4	95.5 ± 1.7	96.2 ± 1.4	96.5 ± 3.1
60	95.6 ± 1.8	97.6 ± 2.1	96.8 ± 0.4	94.4 ± 2.4	94.9 ± 2.5	95.9 ± 2.5
80	94.8 ± 2.5	93.5 ± 2.0	95.8 ± 1.9	93.9 ± 2.9	90.5 ± 3.0	92.9 ± 1.3
100	94.1 ± 4.9	91.6 ± 2.9	94.0 ± 1.6	93.4 ± 2.3	89.4 ± 1.9	91.2 ± 3.0

[a] Three cell lines (HeLa, KB, and FLS) were cultured in the presence of 20−100 μM **LIr1** at 37 °C for 24 and 48 h.

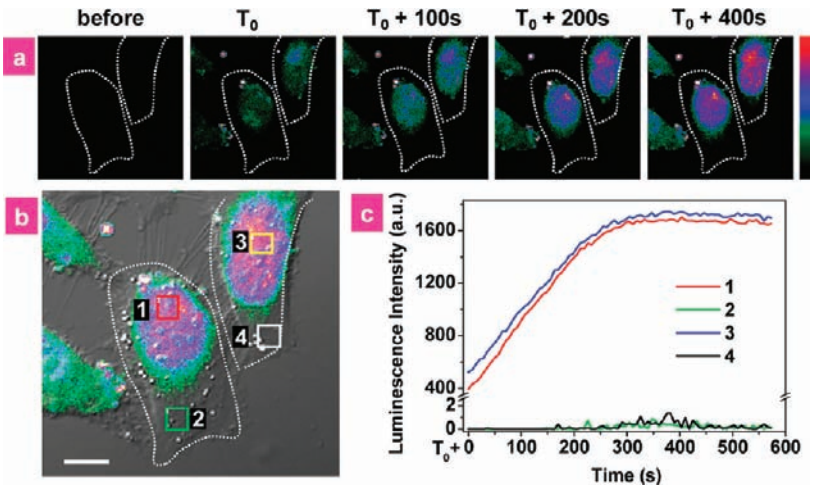

Figure 5. Real-time monitoring of nuclear staining with **LIr1**. Luminescence (a) and bright-field merged (b) images of living HeLa cells incubated with 10 μM **LIr1** in DMSO/PBS (pH 7.4, 1:99, v/v) at 37 °C at selected time points (λ_{ex} = 488 nm, λ_{em} = 520 ± 20 nm; scale bar: 10 μm). T_0 indicates a short time (<30 s) for cells entering the focal plane after **LIr1** was added. (c) Time course of luminescence intensity in the nucleus (regions 1 and 3 in b) and cytoplasm (regions 2 and 4 in b).

of 20−100 μM, the cellular viabilities were estimated to be greater than 94% and 90% (Table 1 and Figure S8 in the Supporting Information) after incubation for 24 and 48 h, respectively. The results indicate that the complex **LIr1** is generally low-toxic for luminescence cellular nuclei imaging (conditions: incubation time of <10 min, **LIr1** concentration of 10 μM). This conclusion was also supported by the result of the Casy Cell Counter and Analyzer System TT under luminescence imaging conditions (Figure S9 in the Supporting Information).

Moreover, to determine the health of the cells after incubation with **LIr1**, a standard live/dead staining procedure using commercially available propidium iodide (PI) was further performed. In a control experiment, when **LIr1**-pretreated HeLa cells were incubated with PI, to which they are normally impermeable, no intracellular fluorescence signal at 600 ± 20 nm was measured in confocal luminescence imaging. This indicated that the PI hardly crossed the cell membrane, and that **LIr1**-pretreated HeLa cells were normal healthy cells. In addition, as determined with trypan blue, the **LIr1**-treated cells retained 97.4 ± 1.1% viability, suggesting low cytotoxicity of **LIr1** at the imaging concentration.

Kinetic Tracking of Cellular Uptake of Complex LIr1. Subsequently, the dynamic process of nuclear staining with **LIr1** was monitored in real time by continuous imaging of living HeLa cells (Figure 5 and movie in Supporting Information). At first, only very weak luminescence was observed in the cells prior to incubation with **LIr1**. However, when the cell culture medium was replaced by a solution containing LIr1, luminescence was detected in the nuclei within a very short period of time (T_0 < 30 s) for cells entering the focal plane of the objective lens (Figure 5a). Thereafter, a continuous increase in luminescence was observed with increasing time. Quantitative analysis of intracellular signal intensities from the cytoplasm and nucleus, respectively, revealed that the addition of **LIr1** triggered a continuous increase in luminescence from the nucleus and that the intensity reached a maximum within 6 min, while the signal from the cytoplasm remained negligible (Figure 5b,c). These data imply that **LIr1** is rapidly internalized by the cells and nuclei, and that specific nuclear staining with **LIr1** can be effectively performed in several minutes, even though **LIr1** lacks a molecular transporter.

Moreover, to reveal the long-term kinetics of **LIr1** internalization, time-lapse imaging was carried out by using a Live Cell Workstation for in situ observation (Figure 6). After incubation with 10 μm **LIr1** for 10 min, the **LIr1**-containing PBS was replaced by fresh DMEM for further culture. Confocal images were then acquired after 0, 15 min, 3 h, 12 h, and 24 h, respectively. As shown in Figure 6, **LIr1** was localized in the cell nuclei over 24 h. Moreover, PI staining showed that the **LIr1**-treated cells were still viable. Interestingly, no significant cell division was observed.

Interaction with Amino Acids and Biomolecules. In the case of **LIr1** with weak emission, the mechanism of nuclear staining

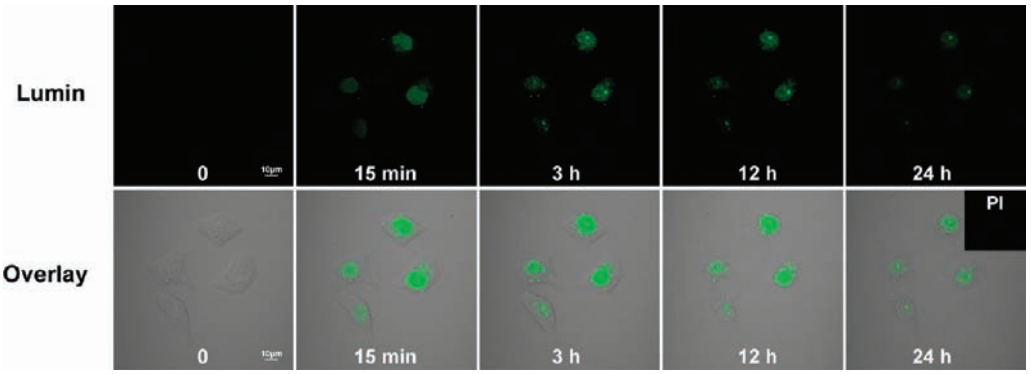

Figure 6. Time-lapse imaging *in situ* of HeLa cells which were preincubated with 10 μM **LIr1** for 10 min and then further cultured in fresh DMEM. Images were acquired after 0, 15 min, 3 h, 12 h, and 24 h, respectively. Inset: PI staining is included to indicate cell viability.

seems to be more complicated. To determine the key factors involved in the luminescence increase upon nuclear staining with **LIr1**, the interactions of **LIr1** with numerous substances in the nucleus, including various amino acids, peptides, deoxyribonucleotide (dNTP), proteins, DNA, and RNA, were examined by luminescence analysis techniques (Figures S10 and S11 in the Supporting Information). The addition of histidine or BSA (as a histidine-rich protein) to **LIr1** triggered a significant luminescence enhancement (Figure S12 in the Supporting Information).[15] For example, the interaction of **LIr1** with histidine resulted in an emission enhancement of >300-fold (Figures S12 and S13 in the Supporting Information), corresponding to a quantum yield of 0.058. The luminescent lifetimes of the adduct of **LIr1** with histidine were measured as ~1.0 and ~0.62 μs in the absence and presence of oxygen, respectively, in phosphate-buffered saline (PBS) (Table S1 in the Supporting Information), which are indicative of the phosphorescent nature of the emission. Besides that, polypeptides (6×His, Pro-Cys-Asn-Glu-Met-Leu, Arg-Trp-Ser-Asp-Thr-Tyr, Val-Gly-Ala-Lys-Gln-Phe), lysozyme (147AA, with one L-histidine residue), and BSA (607AA, with 17 L-histidine residues) with different L-histidine residues were used as examples to investigate contribution of histidine residues to luminescence enhancement of complex **LIr1**. As shown in Figures S14–S16, the addition of these peptides and proteins with different number of histidine residues induced different enhancement in luminescent intensity of **LIr1**. In contrast, weak luminescence changes were observed for the other amino acids, deoxyribonucleotide triphosphate (dNTP), CT DNA, and RNA (Figure S10 in the Supporting Information). Coexistent CT DNA had a negligible interfering effect on the luminescence increase of **LIr1** upon addition of histidine/BSA (Figure S17 in the Supporting Information). As shown in Figure S18 in the Supporting Information, the competitive binding studies of CT DNA and BSA to complex **LIr1** showed that **LIr1** presented high affinity to BSA over CT DNA. Furthermore, comparison of the emission spectrum of **LIr1** in the presence of histidine/BSA (λ_{max}^{em} = ~508 nm) with that obtained for the nuclei of **LIr1**-stained living cells (λ_{max}^{em} = 510 nm; lambda scan by confocal microscopy, Figure S19 in the Supporting Information) revealed that they were very similar in terms of both shape and the maximum emission. Additionally, in a control experiment, when **LIr1** was pretreated with excess histidine (or BSA) and further interacted with living HeLa cells for 25 min, relative weak enhancement in luminescent intensity was observed (Figure S20 in the Supporting Information), which was also confirmed by flow cytometry analysis (Figure S21 in the Supporting Information). All of these facts demonstrate that the intracellular luminescence enhancement is associated with the interaction of **LIr1** with histidine/histidine-containing proteins in the nucleus.

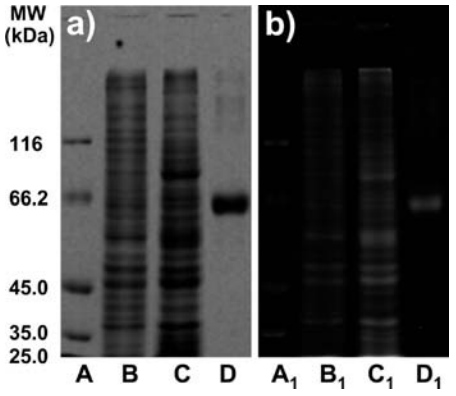

Figure 7. SDS–PAGE analysis of proteins from HeLa cells upon staining with Coomassie brilliant blue complex G-250 and complex **LIr1**. (a) Coomassie brilliant blue G-250 staining. Lanes A–D present protein markers, nuclear proteins, cytoplasm proteins, and BSA, respectively. (b) Complex **LIr1** staining under ultraviolet transillumination. Lanes A_1–D_1 stand for protein markers, nuclear proteins, cytoplasm proteins, and BSA, respectively.

Protein Electrophoresis. To investigate whether this effect of nuclei staining of **LIr1** is associated with distribution of proteins (histidine/histidine-containing) in cells, nuclear and cytoplasmic proteins of HeLa cells were isolated, and then the corresponding protein electrophoresis was carried out. After electrophoresis, the gels were stained with complex **LIr1** (50 μM) for 20 min, and Coomassie Brilliant Blue was used as a reference. As shown in Figure 7, both nuclear and cytoplasmic proteins gave rise to luminescence enhancement of **LIr1**, which is matched with those staining with Coomassie Brilliant Blue, but are slightly different in signal intensity. This result was in well-agreement with imaging result which showed that the fixed cells incubated with **LIr1** displayed a generalized diffuse whole-cell staining pattern (Figure 3b). All these facts demonstrate that the intracellular luminescence enhancement is mainly attributed to the distribution and accumulation of complex **LIr1** in cells rather than the difference of proteins in nuclei and cytoplasm.

Mechanisms of Cellular Uptake. Cellular uptake of small molecules can occur through energy-independent (facilitated

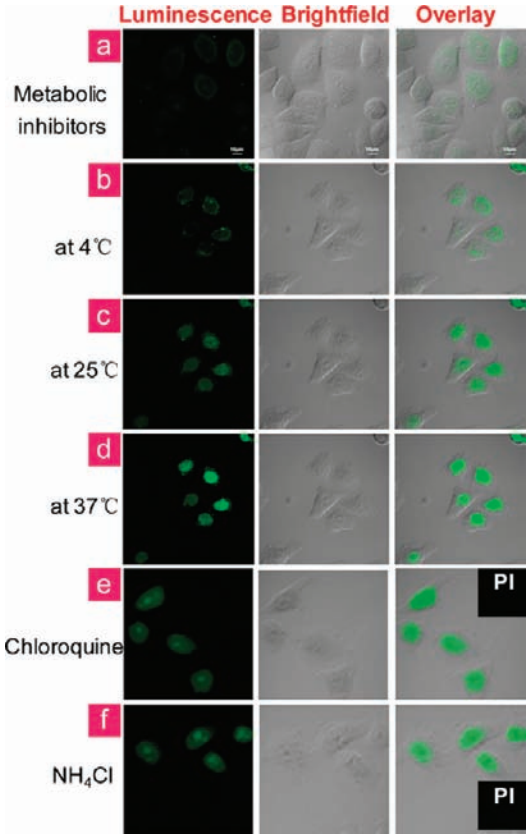

Figure 8. Confocal luminescence image and bright-field images of living HeLa cells incubated with 10 μM **LIr1** in DMSO/PBS (pH 7.4, 1:99, v/v) under different conditions. (a) The cells were preincubated with 50 mM 2-deoxy-D-glucose and 5 μM oligomycin in PBS for 1 h at 37 °C and then incubated with 10 μM **LIr1** at 37 °C for 10 min. (b) The cells were incubated with 10 μM **LIr1** at 4 °C for 10 min. (c and d) As for case b and further incubation at 25 and 37 °C, respectively. (e and f) The cells were pretreated with endocytic inhibitors chloroquine (50 μM) and NH_4Cl (50 mM), respectively, and then incubated with 10 μM **LIr1** at 37 °C for 10 min (λ_{ex} = 488 nm, λ_{em} = 520 ± 20 nm).

diffusion, passive diffusion) and energy-dependent (endocytosis, active transport) pathways. To further explore the cellular and nuclear entry pathway of **LIr1**, **LIr1** staining was investigated in detail under conditions of different temperatures, hypertonic treatment, and in the presence of metabolic and endocytic inhibitors, and the data obtained are shown in Figure 8.

First, the location of **LIr1** was examined when active cellular uptake was blocked by incubation at 4 °C or pretreatment with the metabolic inhibitors 2-deoxy-D-glucose and oligomycin.[21] As determined by confocal luminescence microscopy (Figure 8) and flow cytometry (Figure 9), when active transport was inhibited, the intracellular luminescence was significantly suppressed and prenuclear staining appeared (Figure 8a,b). Interestingly, specific nuclear staining by **LIr1** reappeared (Figure 8c) when the incubation temperature was increased from 4 to 25 °C. With a further increase in the temperature to 37 °C, a continuous enhancement in the luminescence intensity in the nuclear region was measured (Figure 8d). This is not a surprising result when we consider the fact that cell metabolism and physiological activity would be suppressed under low-temperature conditions. These observations suggest that energy plays a very important role in the process of

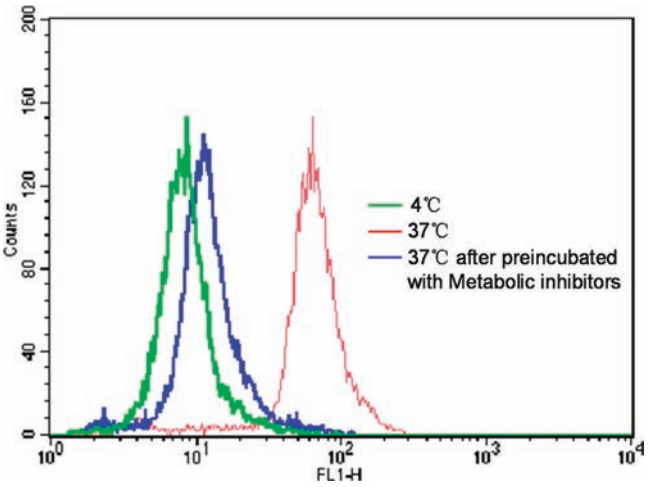

Figure 9. Flow cytometric histogram profile of cellular uptake of **LIr1** in HeLa cells. HeLa cells were incubated with 10 μM **LIr1** in DMSO/PBS (pH 7.4, 1:99, v/v) for 10 min at (red) 37 °C, (green) 4 °C, and (blue) 37 °C after the cells had been preincubated with 50 mM 2-deoxy-D-glucose and 5 μM oligomycin in PBS for 1 h at 37 °C, respectively.

LIr1 crossing the plasma membrane and eventually reaching the nucleus.

Endocytosis is known as a general entry mechanism for various extracellular materials and is an energy-dependent uptake route that can be hindered under conditions of low temperature or adenosine triphosphate (ATP) depletion. Thus, the endocytic inhibitors chloroquine and NH_4Cl were used to assess the contribution of the endocytotic pathway for **LIr1** uptake and entrance into the nuclei of cells. As can be seen from the relative intensities and location of **LIr1** in the cells after treatment with these inhibitors (Figure 8e,f), they had no effect on the ability of **LIr1** to function as a nuclear stain. In addition, the endocytotic pathway is usually a slow process.[22] However, Figure 5c shows that the luminescence intensity in the nucleus reached a maximum within 6 min. The above-mentioned data indicate that the endocytotic pathway is not responsible for the nuclear staining by **LIr1**.

In addition, we also investigated the kinetic diffusion process of **LIr1** in hypertonic solutions of sucrose. In general, concentration gradient, temperature, and osmotic pressure are the three main influencing factors on molecular diffusion. After preincubating HeLa cells with various concentrations of sucrose/PBS solution, the kinetic processes by which **LIr1** crossed the plasma membrane were examined to determine the complex diffusion abilities relative to the control untreated cells. Luminescence intensity and time lapse reached a maximum, indicating that hypertonic treatment had no significant effect on the process of **LIr1** crossing the plasma membrane. However, on increasing the sucrose concentration to 30% (w/v, sucrose/PBS), the maximum luminescence intensity decreased by about 12.8% as compared with that in the control group (Figure 10). This result may be largely attributed to serious intracellular dehydration. As indicated in Figure 9, the luminescence intensity showed no significant variation under the same conditions but in the presence of metabolic inhibitors (37 °C and 37 °C after preincubation with metabolic inhibitors). The data show that diffusion is not the main pathway by which complex LIr1 enters into cells.

The high degree of specificity for living cell nuclear staining by **LIr1** with enhanced luminescence may be ascribed to two

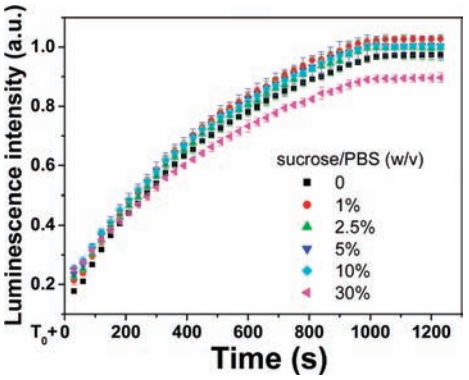

Figure 10. Time courses of luminescence intensity at 520 nm of HeLa cells pretreated with different concentrations of sucrose and then incubated with 10 μM **LIr1** in PBS (pH 7.4) for 10 min at 37 °C.

Scheme 1. Chemical Structure and the Proposed Mechanism of Nuclear Staining with Nonemissive Iridium(III) Complex LIr1[a]

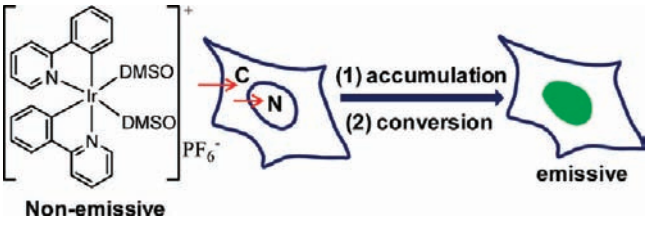

[a] The characters 'C' and 'N' denote cytoplasm and nucleus, respectively.

possible processes: either **LIr1** is evenly distributed in the whole cell, but is only converted to the luminescent form in the nucleus, or **LIr1** is specifically concentrated in the nucleus and then converted into a luminescent product therein. To address this question, the amounts of iridium in the cytoplasm and nucleus of an **LIr1**-stained cell were quantified by ICP-AEC measurement[23] and the result revealed a high ratio between the nucleus (~1.05 pg Ir/cell) and the cytoplasm (<0.08 pg Ir/cell), indicating that more than 93% of the iridium had accumulated in the nucleus. Moreover, when the cells were fixed, the plasma membrane and the nuclear membrane became permeable to **LIr1**, and further incubation with **LIr1** resulted in a generalized diffuse whole-cell staining pattern (Figure 3b), suggesting that **LIr1** was then evenly distributed and converted into the luminescent form in the entire cell. The conclusion was also confirmed by SDS−PAGE gel analysis (Figure 7). Therefore, the specific concentration of the iridium complex in the nucleus is a key factor for the exclusive nuclear staining of living cells with **LIr1**.

On the basis of all of the results obtained above, we propose a possible mechanism of the nuclear staining with **LIr1** as follows: (1) **LIr1** with suitable positive charge and lipophilicity (octanol/water partition coefficient, log $P_{O/W} = -0.12$) readily crosses the cell membrane and accumulates to a great extent in the nucleus, mainly through an energy-dependent mechanism, for example by binding to a transport protein; (2) reactions with histidine/histidine-containing proteins occur immediately to convert the nonemissive complex into a luminescent product in the nucleus (Scheme 1). However, the question as to which protein helps **LIr1** to cross the plasma/nuclear membrane is still under investigation.

CONCLUSION

In summary, we have demonstrated a nonemissive cyclometalated iridium(III) solvent complex **LIr1** as a non-nucleic acid-bonding fluorescence-enhanced nuclear stain that is specifically concentrated in the nuclei of living cells and reacts with histidine/histidine-containing proteins to form a luminescent emissive product in the nuclei. To the best of our knowledge, **LIr1** represents the first reaction-based phosphorescence-enhanced nucleus imaging agent. Its advantages of exclusive nuclear staining of living cells over fixed cells, the very short staining time (<6 min), excitation with visible light (≤488 nm), high signal ratio between the nucleus and the cytoplasm (>200), as well as low cytotoxicity at imaging concentration, without the need for conjugation with a cell-penetrating molecular transporter, promise potential applications of **LIr1** in biomedical research. In particular, the "non-nucleic acid-bonding light-up organelle" design strategy of this nonemissive complex **LIr1**, showing instead a reaction-based mechanism with histidine/histidine-containing proteins, will provide many opportunities for the development of novel agents for living cell-related studies.

ASSOCIATED CONTENT

Supporting Information. Synthesis and experimental details (pdf); movie of nuclear staining with **LIr1** (avi). This material is available free of charge via the Internet at http://pubs.acs.org.

AUTHOR INFORMATION

Corresponding Author
fyli@fudan.edu.cn

ACKNOWLEDGMENT

The authors thank NSFC (20825101 and 91027004), SSTC (10431903100)), IRT0911, SLADP (B108) and the CAS/SAFEA International Partnership Program for Creative Research Teams for financial support.

REFERENCES

(1) Lodish, H.; Berk, A.; Matsudaira, P.; Kaiser, C. A.; Krieger, M.; Scott, M. P.; Zipursky, S. L.; Darnell, J. *Molecular Cell Biology*, 5th ed.; WH Freeman: New York, 2004.

(2) Invitrogen Home pages, www.probes.com and www.invitrogen.com; Haugland, R. P. *A Guide to Fluorescent Probes and Labelling Technologies*, 10th ed.; Molecular Probes: Eugene, OR, 2005; pp 397−405.

(3) Pfeifer, G. P.; You, Y.-H.; Besaratinia, A. *Mutat. Res.* **2005**, *571*, 19–31.

(4) Review on lanthanide complexes for bioimaging: (a) Montgomery, C. P.; Murray, B. S.; New, E. J.; Pal, R.; Parker, D. *Acc. Chem. Res.* **2009**, *42*, 925–937. (b) New, E. J.; Parker, D.; Smith, D. G.; Walton, J. W. *Curr. Opin. Chem. Biol.* **2010**, *14*, 238–246. (c) New, E. J.; Congreve, A; Parker, D. *Chem. Sci.* **2010**, *1*, 111–118. (d) Eliseeva, S. V.; Bünzli, J. C. G. *Chem. Soc. Rev.* **2010**, *39*, 189–227. (e) Bünzli, J. C. G. *Chem. Rev.* **2010**, *110*, 2729–2755.(f) Li, F. Y.; Yang, H.; Hu, H. Charpter 13: Luminescent Rare Earth Complexes as Chemosensors and Biological Probes. In *Rare Earth Coordination Chemistry: Fundamentals and Applications*; Huang, C. H., Ed.; Wiley: Singapore, 2010; pp 525−567.

(5) Recent examples on lanthanide complexes for bioimaging: (a) Yu, J. H.; Pal, R.; Poole, R. A.; Cann, M. J.; Parker, D. *J. Am. Chem.*

Soc. **2006**, *128*, 2294–2300. (b) Pal, R.; Parker, D. *Org. Biomol. Chem.* **2008**, *6*, 1020–1033. (c) Murray, B. S.; New, E. J.; Pal, R.; Parker, D. *Org. Biomol. Chem.* **2008**, *6*, 2085–2094. (d) Montgomery, C. P.; New, E. J.; Palsson, L. O.; Parker, D.; Batsanov, A. S.; Lamarque, L. *Helv. Chim. Acta* **2009**, *92*, 2186–2213. (e) Chauvin, A. S.; Comby, S.; Song, B.; Vandevyver, C. D. B.; Thomas, F.; Bünzli, J. C. G. *Chem.—Eur. J.* **2007**, *13*, 9515–9526. (f) Deiters, E.; Song, B.; Chauvin, A. S.; Vandevyver, C. D. B.; Gumy, F.; Bünzli, J. C. G. *Chem.—Eur. J.* **2009**, *15*, 885–900.

(6) Review on charge-transfer complexes for bioimaging: (a) Zhao, Q.; Huang, C. H.; Li, F. Y. *Chem. Soc. Rev.* **2011**, *40*, 2508–2524. (b) Moreira, V. F.; Greenwood, F. L. T.; Coogan, M. P. *Chem. Commun.* **2010**, *46*, 186–202. (c) Lo, K. K. W.; Li, S. P. Y; Zhang, K. Y. *New J. Chem.* **2011**, *35*, 265–287.

(7) Recent examples on charge-transfer complexes for bioimaging: (a) Zhang, K. Y.; Li, S. P. Y.; Zhu, N. Y.; Or, I. W. S.; Cheung, M. S. H.; Lam, Y. W.; Lo, K. K. W. *Inorg. Chem.* **2010**, *49*, 2530–2540. (b) Leung, S. K.; Kwok, K. Y.; Zhang, K. Y.; Lo, K. K. W. *Inorg. Chem.* **2010**, *49*, 4984–4995. (c) Wu, P.; Wong, E. -M.; Ma, D. -L.; Tong, G. -M.; Ng, K. -M.; Che, C. -M. *Chem.—Eur. J.* **2009**, *15*, 3652–3656. (d) Koo, C. K.; Wong, K. L.; Man, C. W. -Y.; Lam, Y. W.; So, K. Y.; Tam, H. L.; Tsao, S. W.; Cheah, K. W.; Lau, K. C.; Yang, Y. Y.; Chen, J. C.; Lam, M. H. W. *Inorg. Chem.* **2009**, *48*, 872–878. (e) Koo, C. K.; Wong, K. L.; Man, C. W. Y.; Tam, H. L.; Tsao, S. W.; Cheah, K. W.; Lam, M. H. W. *Inorg. Chem.* **2009**, *48*, 7501–7503. (f) Koo, C. K.; Leo, K. Y.; Wong, K. L.; Ho, Y. M.; Lam, Y. W.; Lam, M. H. W.; Cheah, K. W.; Cheng, C. W.; Kwok, W. M. *Chem.—Eur. J.* **2010**, *16*, 3942–3950. (g) Zhao, Q.; Zhao, Y. M. X.; Shi, L. X.; Liu, S. J.; Li, C. Y.; Shi, M.; Zhou, Z. G.; Huang, C. H.; Li, F. Y. *Organometallics* **2010**, *29*, 1085–1091. (h) Xiong, L. Q.; Zhao, Q.; Chen, H. L.; Wu, Y. B.; Dong, Z. S.; Zhou, Z. G.; Li, F. Y. *Inorg. Chem.* **2010**, *49*, 6402–6408. (i) Wu, H. Z.; Yang, T. S.; Zhao, Q.; Zhou, J.; Li, C. Y.; Li, F. Y. *Dalton Trans.* **2011**, *40*, 1969–1976. (j) Yang, T. S.; Xia, A.; Liu, Q.; Shi, M.; Wu, H. Z.; Xiong, L. Q.; Huang, C. H.; Li, F. Y. *J. Mater. Chem.* **2011**, *21*, 5360–5367.

(8) Yu, M. X.; Zhao, Q.; Shi, L. X.; Li, F. Y.; Zhou, Z. G.; Yang, H.; Yi, T.; Huang, C. H. *Chem. Commun.* **2008**, 2115–2117.

(9) (a) Chi, Y.; Chou, P. T. *Chem. Soc. Rev.* **2010**, *39*, 638. (b) Zhao, Q.; Li, F. Y.; Huang, C. H. *Chem. Soc. Rev.* **2010**, *39*, 3007–3030.

(10) (a) Hanaoka, K.; Kikuchi, K.; Kobayashi, S.; Nagano, T. *J. Am. Chem. Soc.* **2007**, *129*, 13502–13509. (b) Botchway, S. W.; Charnley, M.; Haycock, J. W.; Parker, Q. W.; Rochester, D. L.; Weinstein, J. A.; Williams, J. A. G. *Proc. Natl. Acad. Sci. U.S.A.* **2008**, *105*, 16071. (c) Murphy, L.; Congreve, A.; Pålsson, L. O.; Williams, J. A. G. *Chem. Commun.* **2010**, *46*, 8743–8745.

(11) Law, G. L.; Man, C.; Parker, D.; Walton, J. W. *Chem. Commu.* **2010**, *46*, 2391–2393.

(12) Puckett, C. A.; Barton, J. K. *J. Am. Chem. Soc.* **2009**, *131*, 8738–8739.

(13) Gill, M. R.; Garcia-Lara, J.; Foster, S. J.; Smythe, C.; Battaglia, G.; Thomas, J. A. *Nat. Chem.* **2009**, *1*, 662–667.

(14) Nonoyama, K. *Bull. Chem. Soc. Jpn.* **1974**, *47*, 467–468.

(15) Schmid, B.; Garces, F. O.; Watts, R. J. *Inorg. Chem.* **1994**, *33*, 9–14.

(16) Tan, W. J.; Zhang, Q.; Zhang, J. J.; Tian, H. *Org. Lett.* **2009**, *11*, 161–164.

(17) (a) Minick, D. J.; Frenz, J. H.; Patrick, M. A.; Brent, D. A. *J. Med. Chem.* **1988**, *31*, 1923–1933.(b) Sansgter, J. *Octanol-Water Partition Coefficients: Fundamentals and Physical Chemistry*; Wiley: Chichester, 1997.

(18) Yu, M. X.; Li, F. Y.; Chen, Z. G.; Hu, H.; Zhan, C.; Yang, H.; Huang, C. H. *Anal. Chem.* **2009**, *81*, 930–935.

(19) Serroni, S.; Juris, A.; Campagna, S.; Venturi, M.; Denti, G.; Balzani, V. *J. Am. Chem. Soc.* **1994**, *116*, 9086–9091. (b) Calogero, G.; Giuffrida, G.; Serroni, S.; Ricevuto, V.; Campagna, S. *Inorg. Chem.* **1995**, *34*, 541–545. (c) Mamo, A.; Stefio, I.; Parisi, M. F.; Credi, A.; Venturi, M.; Di Pietro, C.; Campagna, S. *Inorg. Chem.* **1997**, *36*, 5947–5950.

(20) Ma, D. L.; Wong, W. L.; Chung, W. H.; Chan, F. Y.; So, P. K.; Lai, T. S.; Zhou, Z. Y.; Leung, Y. C.; Wong, K. Y. *Angew. Chem., Int. Ed.* **2008**, *47*, 3735–3739.

(21) (a) Puckett, C. A.; Barton, J. K. *Biochemistry* **2008**, *47*, 11711–11716. (b) Zhang, K. Y.; Lo, K. K. W. *Inorg. Chem.* **2009**, *48*, 6011–6025. (c) Zhang, K. Y.; Liu, H. W.; Fong, T. T.-H.; Chen, X. G.; Lo, K. K. W. *Inorg. Chem.* **2010**, *49*, 5432–5443.

(22) (a) Cartiera, M. S.; Johnson, K. M.; Rajendran, V.; Caplan, M. J.; Saltzman, W. M. *Biomaterials* **2009**, *30*, 2790–2798. (b) Jin, H.; Heller, D. A.; Strano, M. S. *Nano Lett.* **2008**, *8*, 1577–1585.

(23) Louie, M. W.; Liu, H. W.; Lam, M. H. C.; Lau, T.-C.; Lo, K. K. W. *Organometallics* **2009**, *28*, 4297–4307.